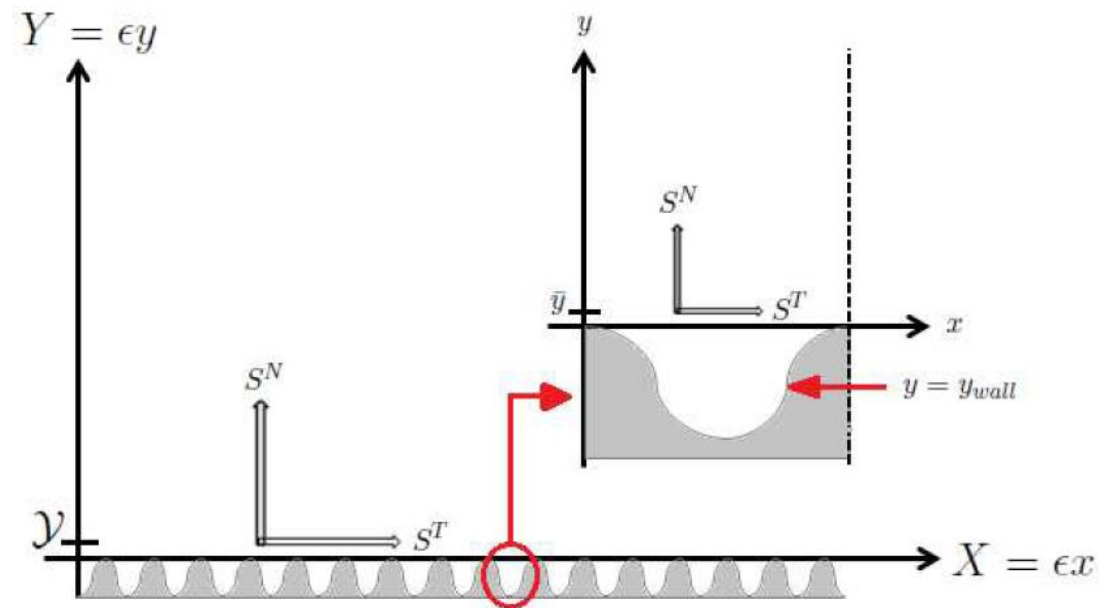




Effective boundary conditions at a regularly micro-structured wall: a second-order homogenization approach



Based on joint work with Sahrish B. Naqvi.



(the smooth wall)

Si elle était perpendiculaire à l'axe des y ,

$$Eu + \varepsilon \frac{du}{dy} = 0, Ew + \varepsilon \frac{dw}{dy} = 0;$$

La valeur de la constante E doit varier suivant la nature des corps avec lesquels le fluide est en contact, et (ce qui est physiquement impossible) s'il y avait un espace vide au-dessus de la portion libre de la surface du fluide, ces équations devraient encore être satisfaites pour les points appartenant à cette portion, en y supposant $\bar{E} = 0$.

.... la constante ε représente en unités de poids la résistance provenant du glissement de deux couches quelconques l'une sur l'autre, pour une étendue égale à l'unité superficielle.

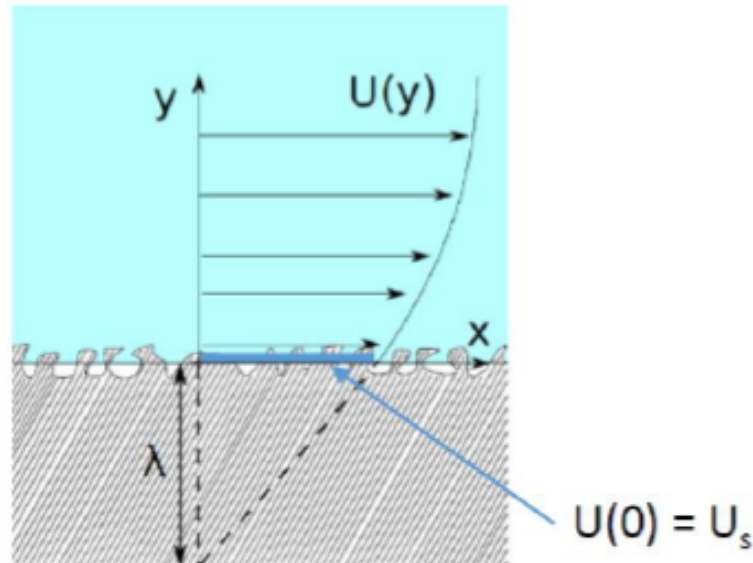
Henri Navier, 1823





In today's words and terminology, Navier's argument was that there is *partial slip*, and the resistance of the wall is proportional to the slip velocity U_s :

$$E U_s = -\varepsilon \left. \frac{dU}{dy} \right|_{y=0} \rightarrow U(0) = (-\varepsilon/E) \left. \frac{dU}{dy} \right|_{y=0} = \lambda \left. \frac{dU}{dy} \right|_{y=0}$$



λ = slip length



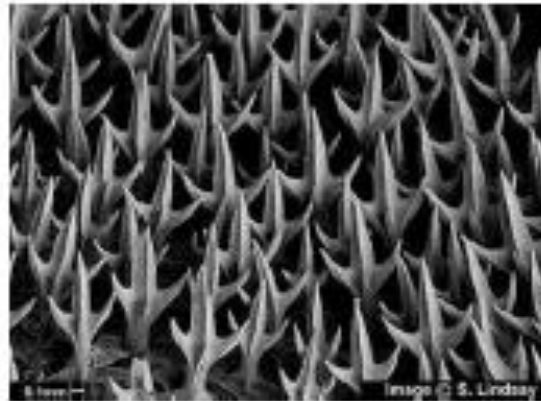
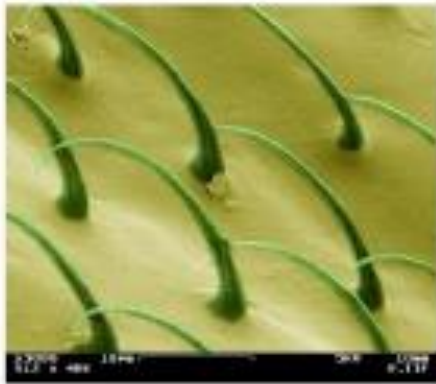
- Navier's slip condition is a first-order development around a fictitious wall (the position $y = 0$ is arbitrary) applicable when either
 - (i) the surface geometry is microstructured or
 - (ii) the continuum approximation breaks down.
- There is a unique slip length λ for U and W only for isotropic (in x, z) walls. The general (anisotropic) case requires (to first order) that:

$$\begin{bmatrix} U(x, 0, z) \\ W(x, 0, z) \end{bmatrix} = \Lambda \frac{\partial}{\partial y} \begin{bmatrix} U(x, 0, z) \\ W(x, 0, z) \end{bmatrix},$$

with Λ a slip tensor (plus a *non-penetration* condition for V).



Irregular surfaces are the norm, not the exception





Literature has always turned around the (first order) Navier slip condition, for both regularly microstructured walls and random roughness (with few exceptions):

Achdou, Pironneau & Valentin,
Jäger & Mikelić,

Basson & Gérard-Varet,

Kamrin, Bazant & Stone,

Luchini,

Introïni, Quintard & Duval,

Guo, Vera-Tissoires & Quintard,

Jimenez-Bolanos & Vernescu,

Zampogna, Magnaudet & Bottaro,

Lacis et al.,

J. Comp. Phys. 1996

J. Diff. Equations 2001

Comm. Pure Appl. Math. 2008

J. Fluid Mech. 2010

J. Fluid Mech. 2013

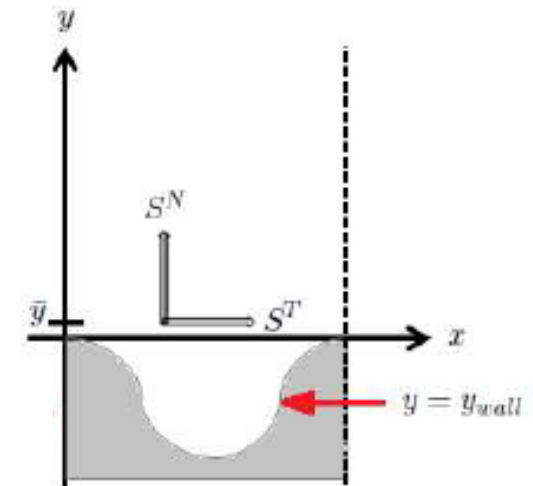
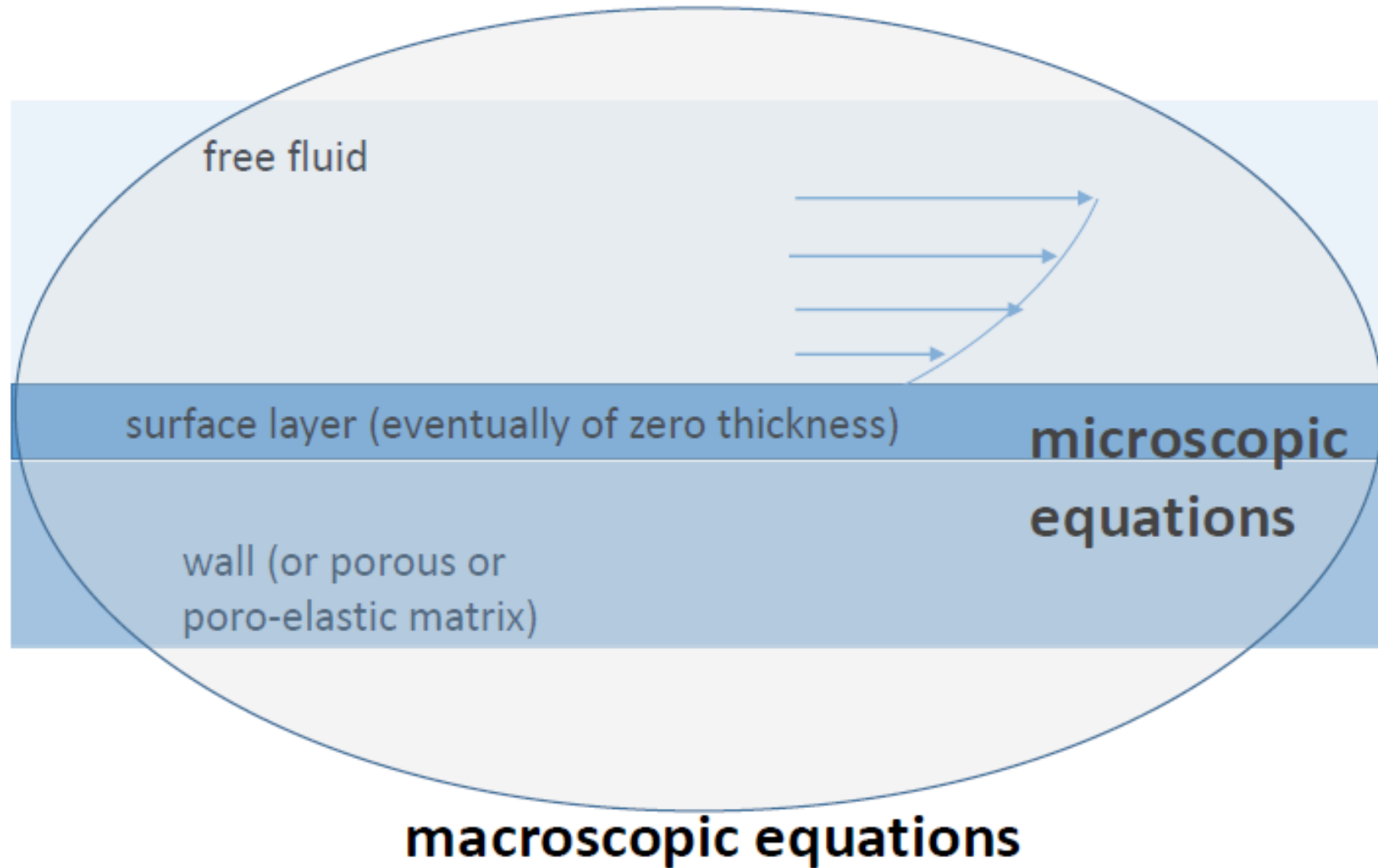
Int. J. Heat Mass Transf. 2011

J. Comp. Phys. 2016

Phys. Fluids 2017

J. Fluid Mech., 2019

J. Fluid Mech., in press



unit cell



Microscopic equations:

$$u_x + v_y = 0,$$

$$\mathcal{R}(u_t + \mathbf{u} \cdot \nabla u) = -p_x + \nabla^2 u + f^x,$$

$$\mathcal{R}(v_t + \mathbf{u} \cdot \nabla v) = -p_y + \nabla^2 v + f^y,$$

$$\mathcal{R} = \rho U l / \mu$$

Macroscopic equations:

$$U_X + V_Y = 0,$$

$$U_T + \mathbf{U} \cdot \nabla' U = -P_X + Re^{-1}(U_{XX} + U_{YY}),$$

$$V_T + \mathbf{U} \cdot \nabla' V = -P_Y + Re^{-1}(V_{XX} + V_{YY}),$$

$$Re = \rho U_{out} L / \mu.$$



$$\mathcal{U} = \epsilon U_{out}$$



$$\mathcal{R} = \epsilon^2 Re$$

$$\epsilon = l/L$$

Power series expansion
for microscopic variables:

$$f = f^{(0)} + \epsilon f^{(1)} + \epsilon^2 f^{(2)} + \dots,$$

$$\nabla \rightarrow \nabla + \epsilon \nabla'$$



Microscopic system at leading order:

Homogeneous Stokes equations, plus periodicity in x , plus no-slip at the wall, plus forcing from the outer flow

$$u_y^{(0)} + v_x^{(0)} = \mathcal{S}^T, \quad -p^{(0)} + 2v_y^{(0)} = \mathcal{S}^N$$

at the edge of the unit cell ($y = y_\infty$).



Microscopic system at next order:

$$\begin{aligned}u_x^{(1)} + v_y^{(1)} &= -u_X^{(0)} - v_Y^{(0)}, \\-p_x^{(1)} + u_{xx}^{(1)} + u_{yy}^{(1)} &= p_X^{(0)} - 2u_{Xx}^{(0)} - 2u_{Yy}^{(0)}, \\-p_y^{(1)} + v_{xx}^{(1)} + v_{yy}^{(1)} &= p_Y^{(0)} - 2v_{Xx}^{(0)} - 2v_{Yy}^{(0)}.\end{aligned}$$

plus boundary conditions.



Linearity permits to express the order zero solution as

$$u^{(0)} = u^\dagger(x, y) \mathbb{S}^T,$$

$$v^{(0)} = v^\dagger(x, y) \mathbb{S}^T,$$

$$p^{(0)} = p^\dagger(x, y) \mathbb{S}^T - \mathbb{S}^N.$$

so that a Stokes system for the ‘dagger’ variables ensues with

$$u_y^\dagger + v_x^\dagger = 1, \quad -p^\dagger + 2v_y^\dagger = 0$$

at y_∞

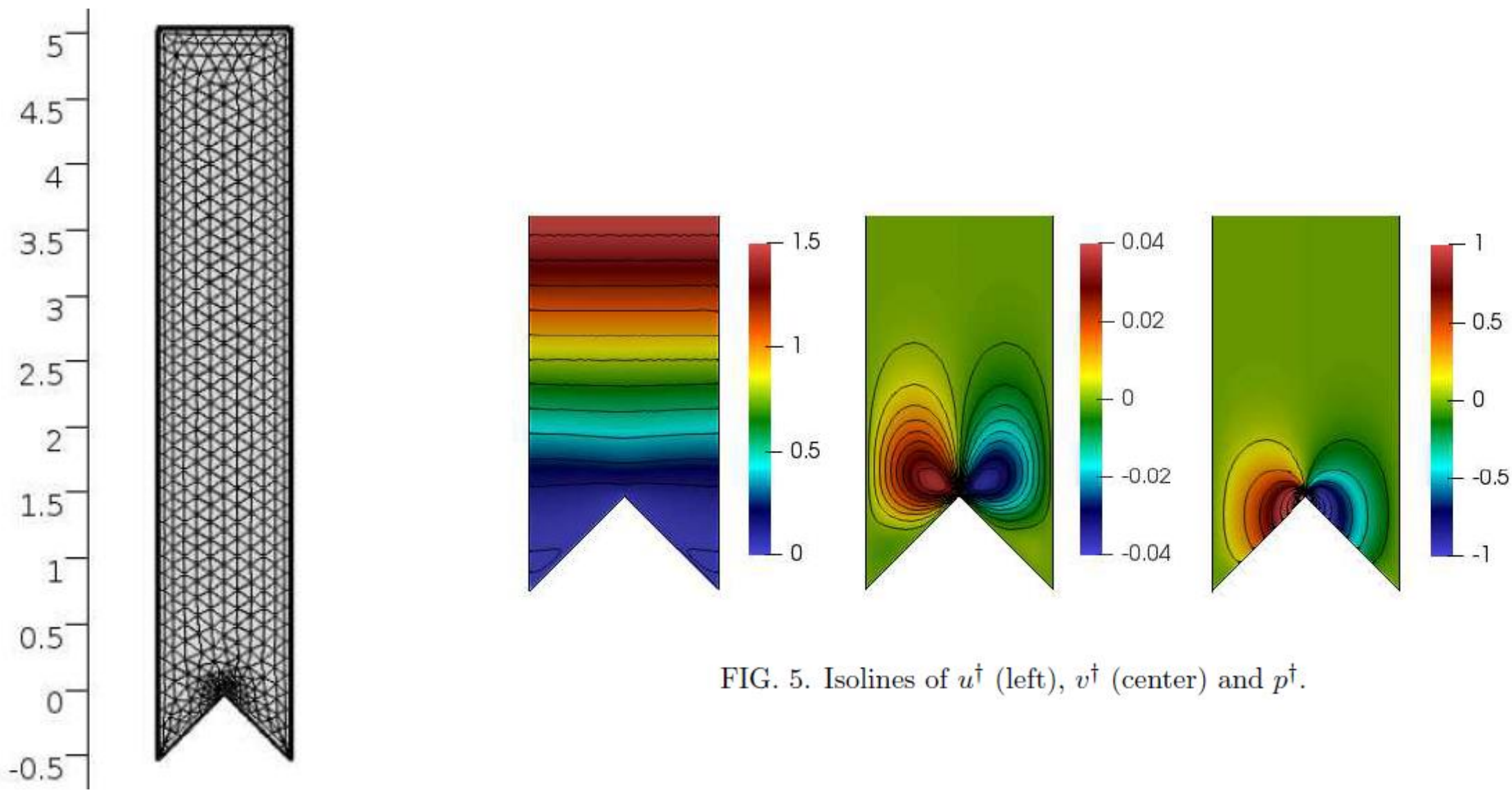


FIG. 5. Isolines of u^\dagger (left), v^\dagger (center) and p^\dagger .



- At order one the system becomes

$$u_x^{(1)} + v_y^{(1)} = -u^\dagger \mathcal{S}_X^T,$$

$$-p_x^{(1)} + u_{xx}^{(1)} + u_{yy}^{(1)} = p^\dagger \mathcal{S}_X^T - \mathcal{S}_X^N - 2u_x^\dagger \mathcal{S}_X^T,$$

$$-p_y^{(1)} + v_{xx}^{(1)} + v_{yy}^{(1)} = -2v_x^\dagger \mathcal{S}_X^T,$$

and the generic solution reads:

$$f^{(1)} = \hat{f}(x, y) \mathcal{S}_X^T + \check{f}(x, y) \mathcal{S}_X^N$$



Forcing by X-gradient of shear stress

$$\begin{aligned}\hat{u}_x + \hat{v}_y &= -u^\dagger, \\ -\hat{p}_x + \hat{u}_{xx} + \hat{u}_{yy} &= p^\dagger - 2u_x^\dagger, \\ -\hat{p}_y + \hat{v}_{xx} + \hat{v}_{yy} &= -2v_x^\dagger.\end{aligned}$$

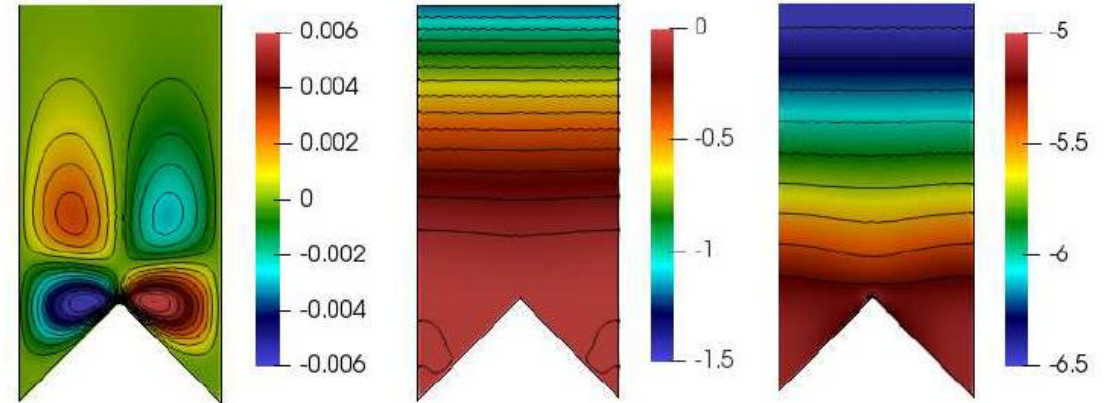


FIG. 6. Isolines of \hat{u} (left), \hat{v} (center) and \hat{p} .



Forcing by X-gradient of normal stress

$$\check{u}_x + \check{v}_y = 0,$$

$$-\check{p}_x + \check{u}_{xx} + \check{u}_{yy} = -1,$$

$$-\check{p}_y + \check{v}_{xx} + \check{v}_{yy} = 0,$$

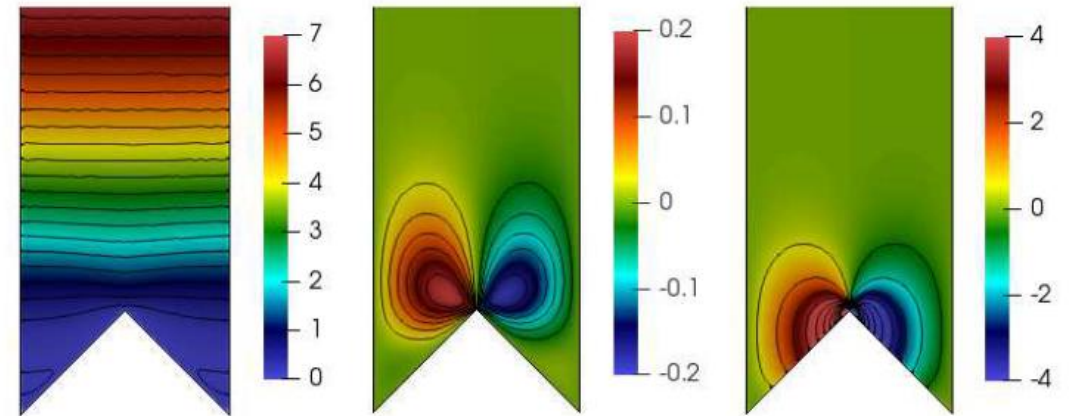


FIG. 7. Isolines of \check{u} (left), \check{v} (center) and \check{p} .



The **macro**scopic effective conditions at $Y_\infty = \epsilon y_\infty$ are:

$$U(X, \epsilon y_\infty, t) = \epsilon \left[\int_0^1 (u^{(0)} + \epsilon u^{(1)}) \Big|_{y=y_\infty} dx \right] + \mathcal{O}(\epsilon^3),$$
$$V(X, \epsilon y_\infty, t) = \epsilon \left[\int_0^1 (v^{(0)} + \epsilon v^{(1)}) \Big|_{y=y_\infty} dx \right] + \mathcal{O}(\epsilon^3).$$



i.e.

$$U(X, \epsilon y_\infty, t) \approx \epsilon \gamma_x S^T + \epsilon^2 n_{12} S_X^N,$$
$$V(X, \epsilon y_\infty, t) \approx \epsilon^2 n_{21} S_X^T.$$

and, for $y_\infty = 5$, we find

$$\gamma_x := \int_0^1 u^\dagger(x, y_\infty) dx = 5.07778$$

$$n_{12} := \int_0^1 \check{u}(x, y_\infty) dx = 12.89469$$

$$n_{21} := \int_0^1 \hat{v}(x, y_\infty) dx = -12.89469$$



y_∞	4	5	6	7	8	9
γ_x	4.07778	5.07778	6.07778	7.07778	8.07778	9.07778
$n_{12} = -n_{21}$	8.31693	12.89469	18.47249	25.05028	32.62806	41.20585

TABLE I. Variation of coefficients with the position of the inner domain's edge.

$$n_{12} = -n_{21} = \frac{y_\infty^2}{2} + \lambda_x y_\infty + m_{12},$$
$$\gamma_x = \frac{dn_{12}}{dy_\infty} = y_\infty + \lambda_x,$$

with $\lambda_x = 0.07778$ and $m_{12} = -m_{21} = 0.00581$.



It is thus convenient to transfer the conditions to $Y = 0$, rim of the roughness elements, i.e.

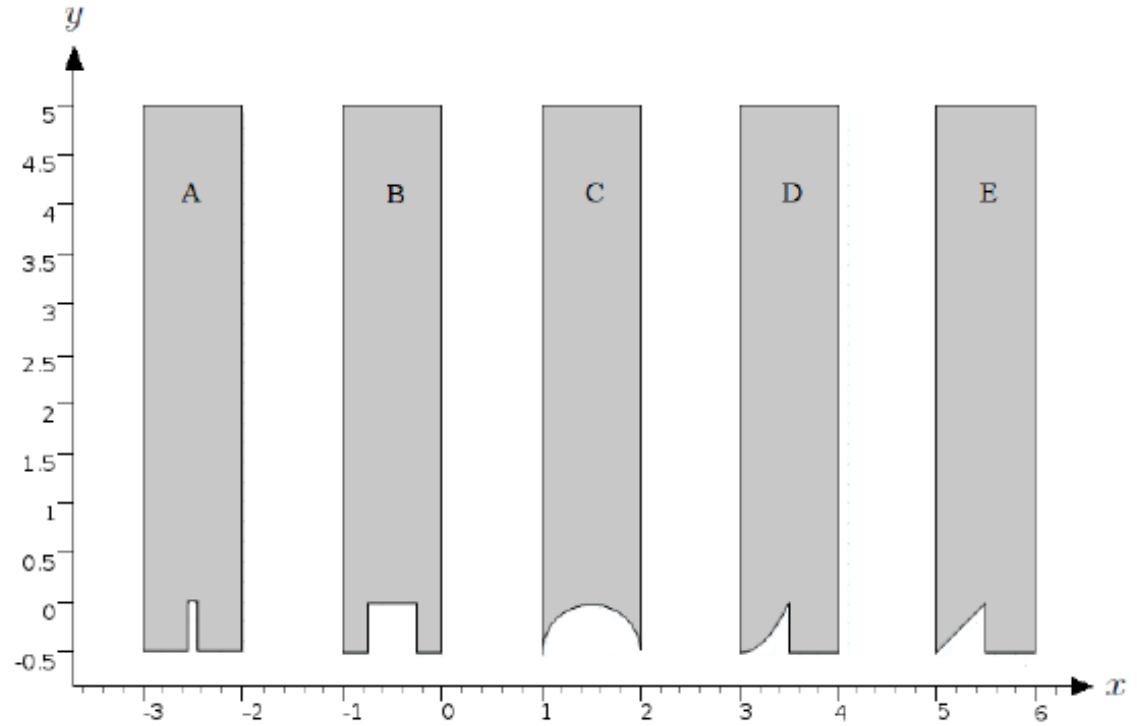
$$U(X, 0, t) = \epsilon \lambda_x S^T + \epsilon^2 m_{12} S_X^N + \mathcal{O}(\epsilon^3)$$

$$V(X, 0, t) = \epsilon^2 m_{21} S_X^T + \mathcal{O}(\epsilon^3)$$

with $S^T = U_Y + V_X$, $S^N = -ReP + 2V_Y$, evaluated at $Y = 0$



Other roughness shapes:



	A	B	C	D	E
λ_x	0.06293	0.01781	0.04087	0.08119	0.07992
$m_{12} = -m_{21}$	0.00324	0.00042	0.00183	0.00546	0.00550

TABLE II. Variation of slip and transpiration parameters for different roughness geometries.



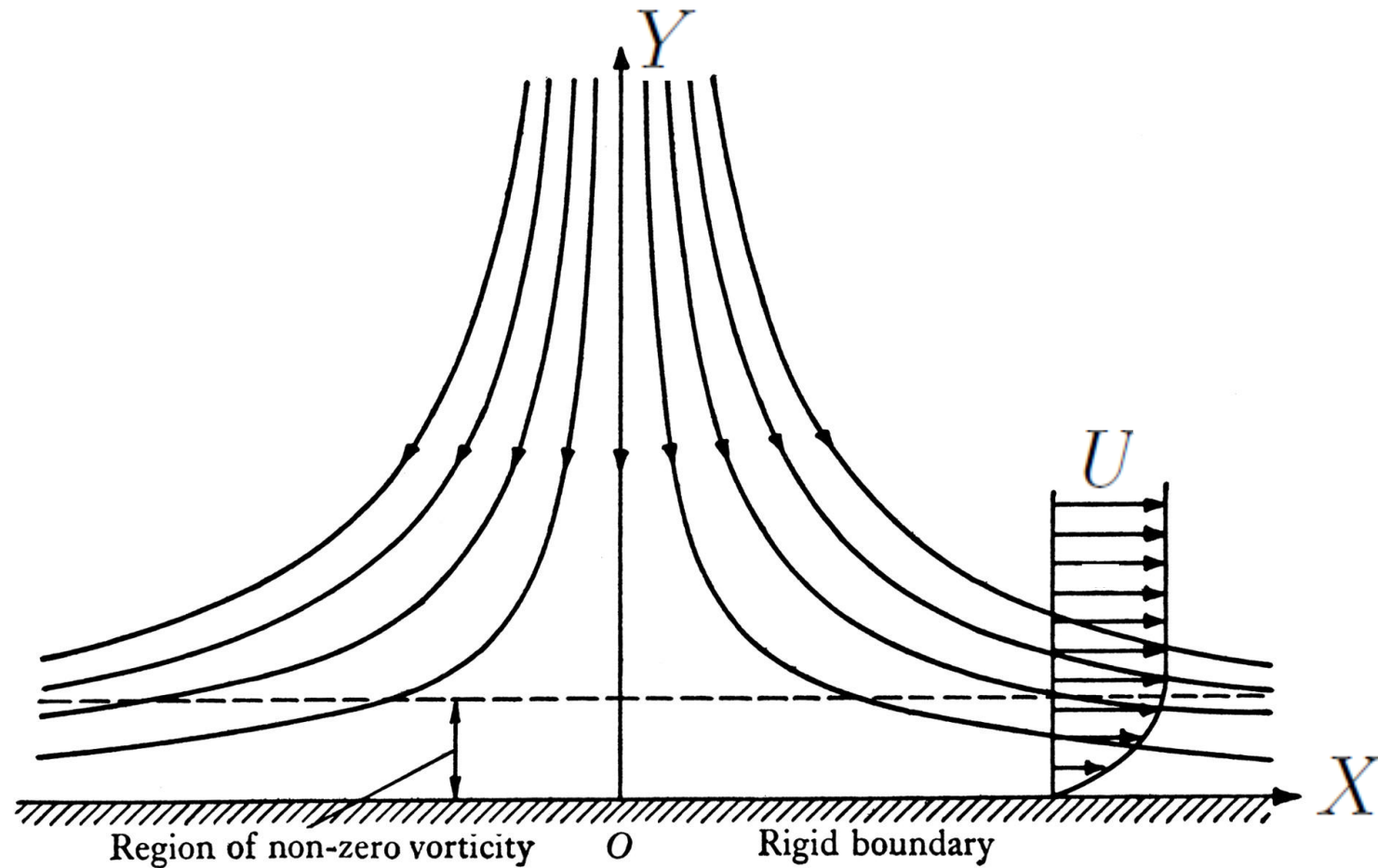
Università
di Genova

DICCA DIPARTIMENTO
DI INGEGNERIA CIVILE, CHIMICA
E AMBIENTALE

Macroscopic test



Macroscopic test: the Hiemenz stagnation point flow





Rough Hiemenz flow:

a *similarity solution* exists also when roughness is present

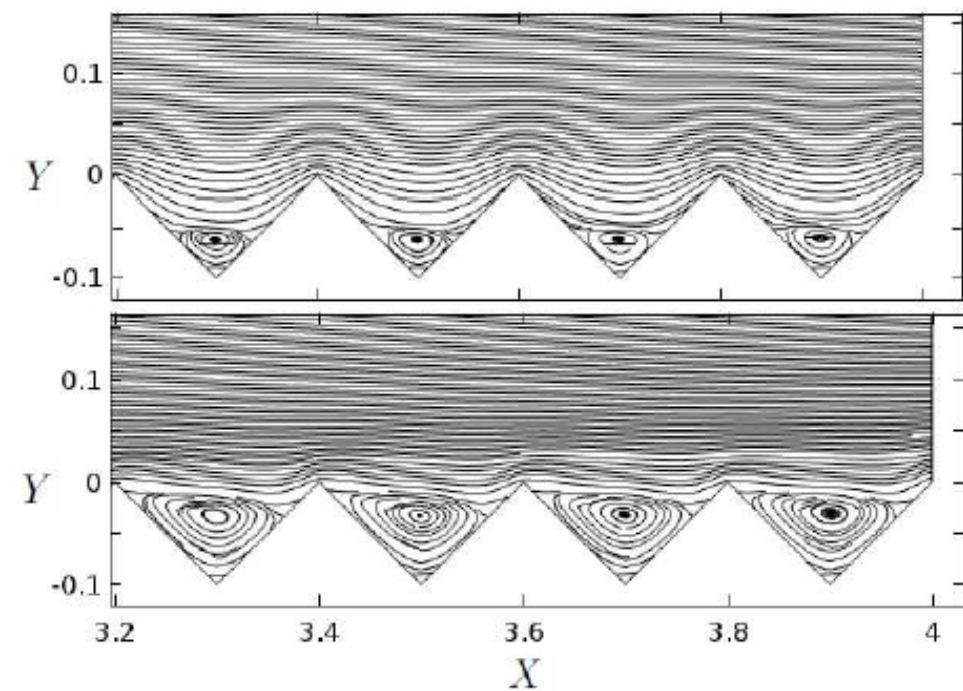
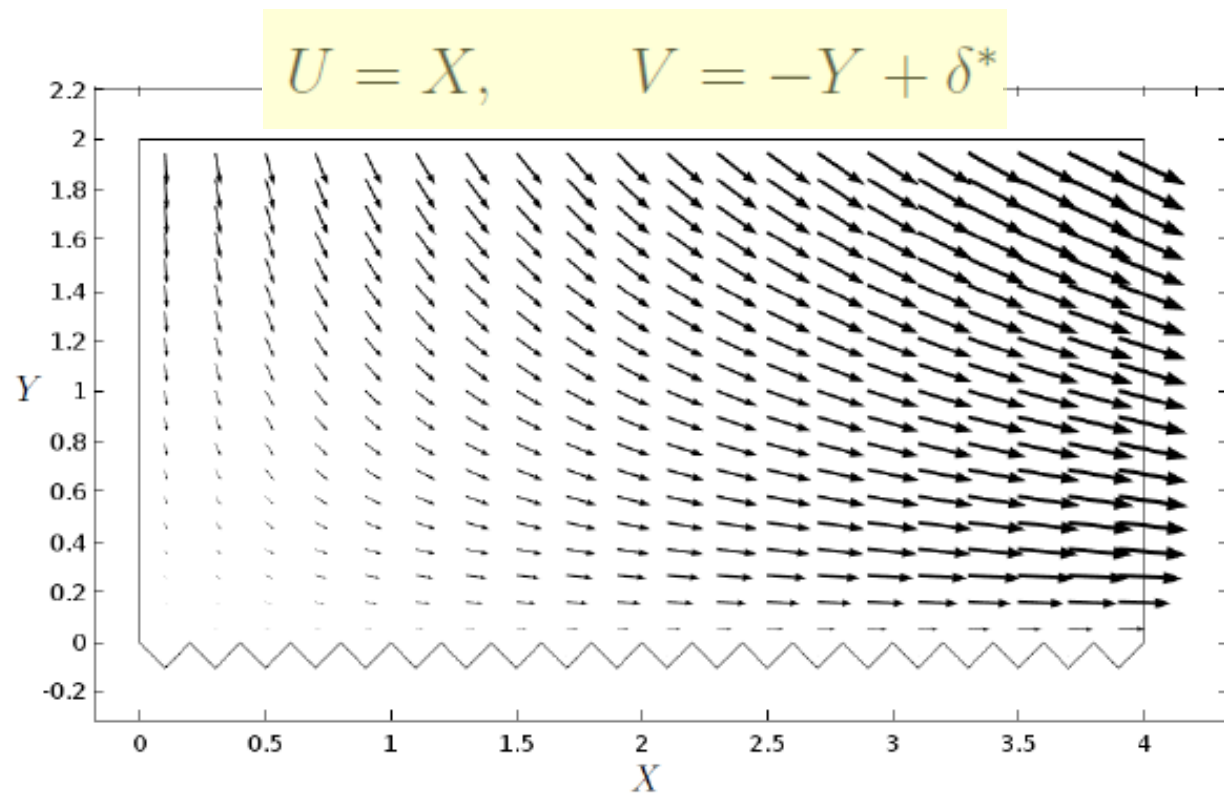
$$U = X f'(Y), \quad V = -f(Y), \quad P = P_0 - \frac{1}{2} [X^2 + g(Y)]$$

$$\frac{1}{Re} f''' + f f'' - f'^2 + 1 = 0,$$

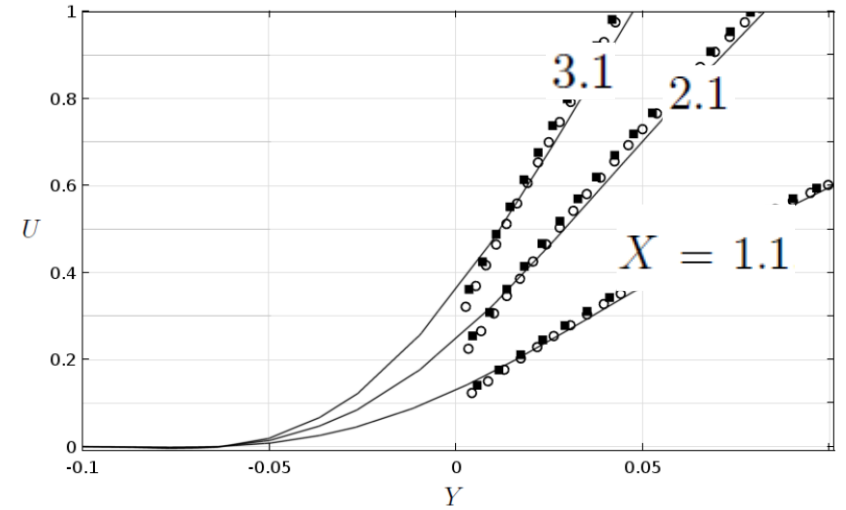
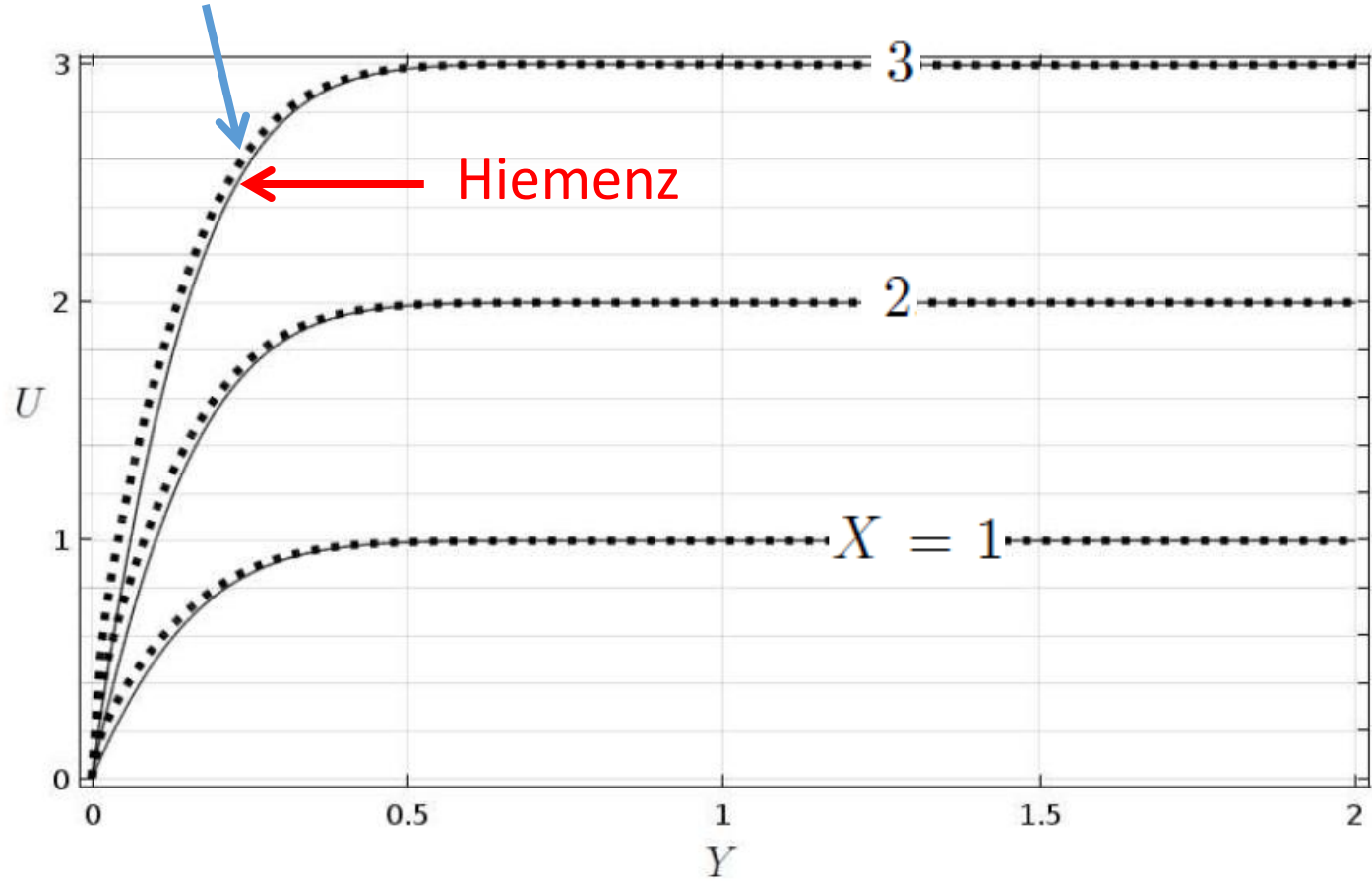
$$\epsilon \lambda_x f'' - f' + \epsilon^2 m_{12} Re = 0, \quad \epsilon^2 m_{21} f'' + f = 0 \quad \text{at} \quad Y = 0,$$

$$f' = 1 \quad \text{at} \quad Y \rightarrow \infty,$$

FreeFEM numerical resolution: $Re = 25, \epsilon = 0.2, \mathcal{R} = \epsilon^2 Re = 1$

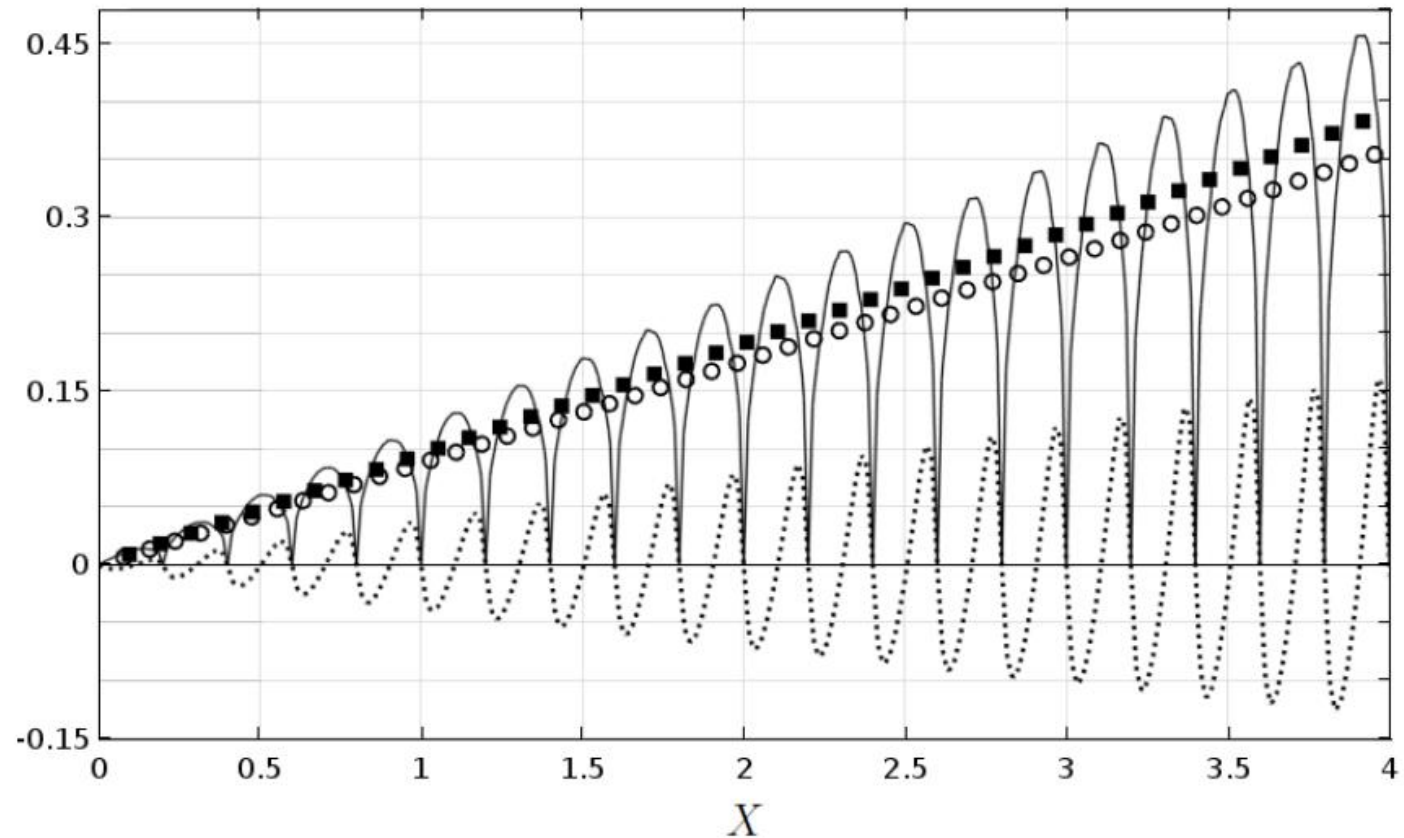


rough Hiemenz





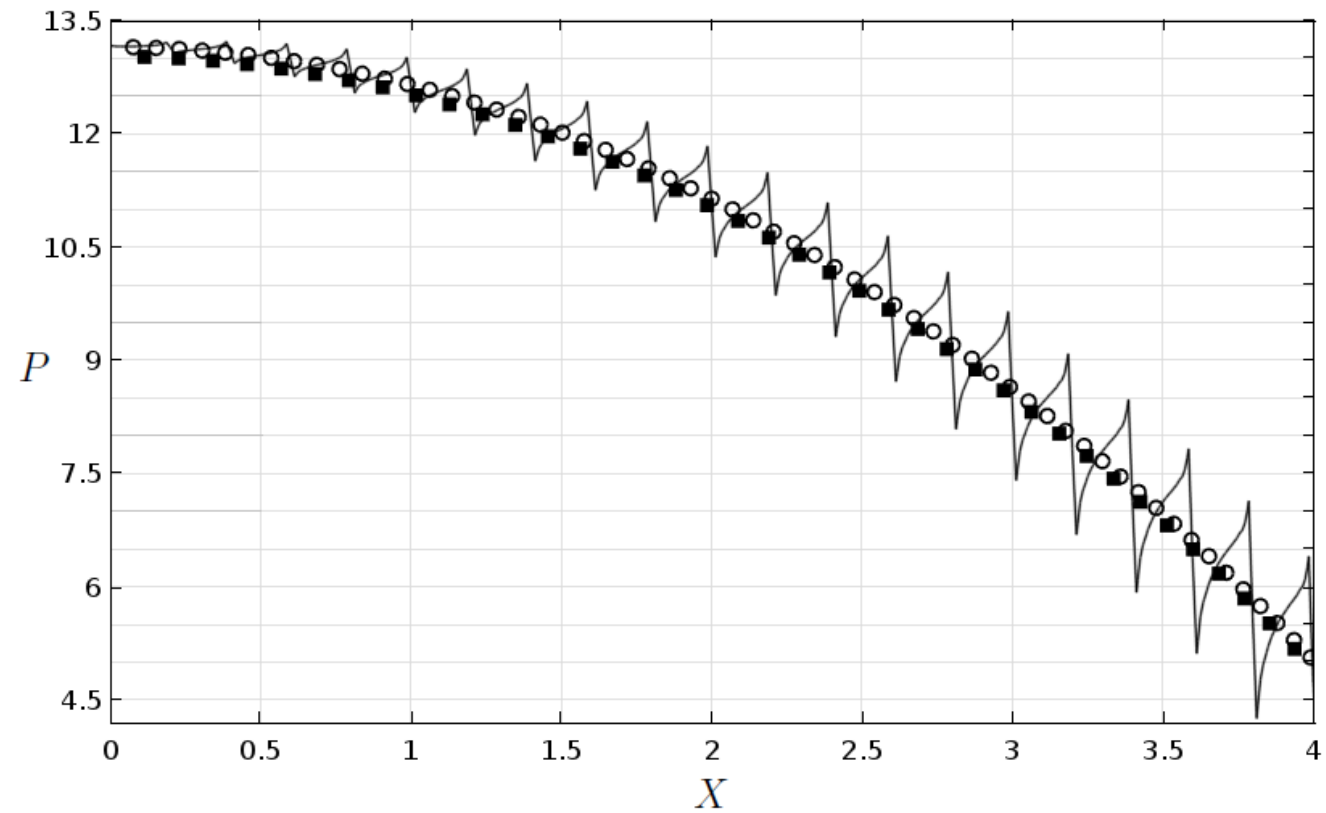
slip and transpiration velocity components



(appreciable difference between the solutions at order ε and ε^2)



pressure at $Y = 0$



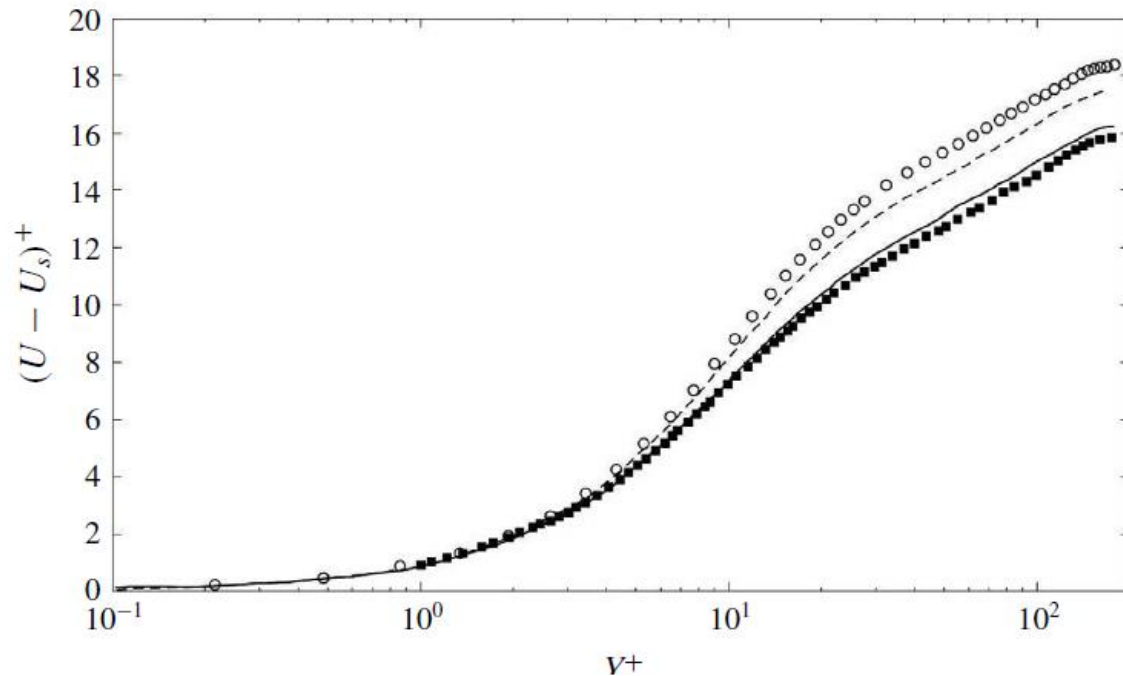


Larger differences between the order 1 and 2 conditions are expected for the case of 3D, laminar or turbulent flow cases

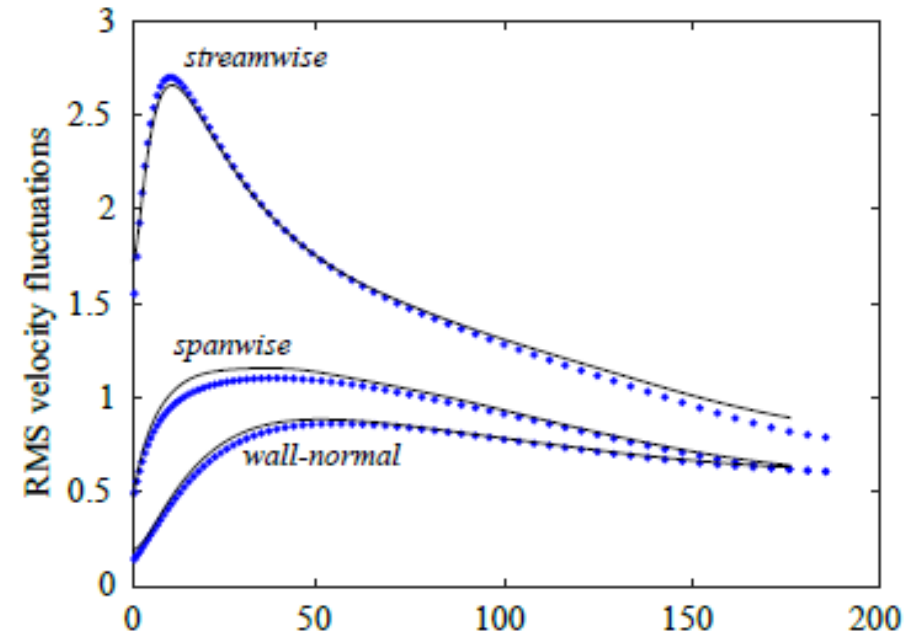


In a three-dimensional turbulent channel flow with a rough wall the transpiration condition seems to work well (cuboid roughness, $\varepsilon = 0.2$) ...

Flow over natural or engineered surfaces



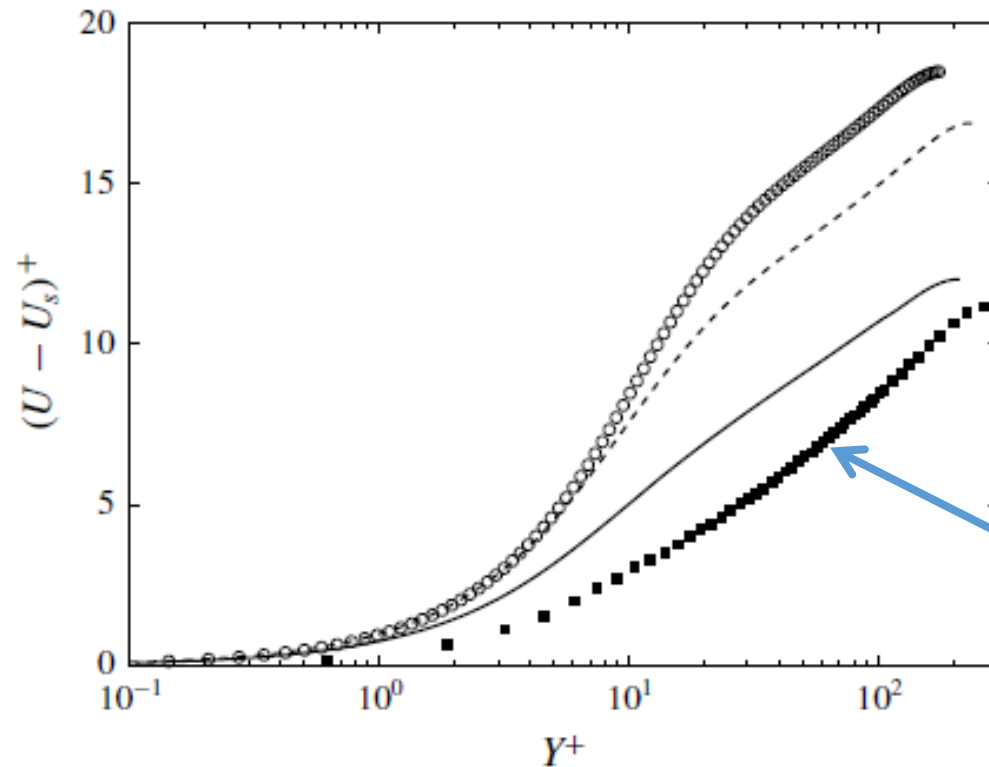
Bottaro, *J. Fluid Mech.* 2019



Lacis et al., *J. Fluid Mech.* in press



... although this is not always true (cubic roughness elements, $\varepsilon = 0.4$) ...



feature-resolving simulations
by Orlandi & Leonardi,
J. Turbulence 2006

BUT ...



BUT ...

in the models used above (both Bottaro and Lacis et al.) the conditions used at the fictitious wall in $Y = 0$ are first order for U (i.e. simple Navier slip) and second order for V .

Need to do: DNS with second order conditions throughout



Summary

1. Developed second order conditions to be employed at a fictitious wall to model a micro-structured wall
2. Very simple to extract coefficients of the second order conditions by solving as few as two Stokes-like equations in unit cells of different heights and extrapolating results to $y_{\infty} = 0$
3. Conditions is formally correct for $\varepsilon \rightarrow 0$, but results seem to be acceptable for rather large values of ε
4. Trivial extension to 3D roughness



Future developments (SHS/LIS):

1. include a lubricant fluid within the roughness (VOF in unit cell)
2. derive slip/transpiration conditions to second order in this two-phase flow case (1st order problem already solved using BEM: Alinovi & Bottaro, *Phys. Rev. Fluids*, 2018)
3. perform DNS with slip/transpiration for turbulent channel flow over a LIS and compare to feature-resolving DNS
4. optimise morphology of rough surface impregnated with lubricant and optimise properties of lubricant fluid